Thermal Stress Analysis of Concrete Bridge Superstructures

M. Radolli, M. M. Dillon Ltd., Cambridge, Ontario
R. Green, Department of Civil Engineering, University of Waterloo, Ontario

Only mean temperature changes are generally considered in the design of concrete bridge superstructures. Because of daily changes in both ambient temperature and intensity of solar radiation, temperature differentials also exist in concrete superstructures. These temperature differentials induce stresses throughout the depth of concrete structures, which are generally not included in current design procedures. This paper describes the heat transfer processes that occur between the atmosphere and a concrete superstructure and also the climatic conditions necessary for the development of temperature differentials during both summer and winter. Temperature-time analyses, computed by using a one-dimensional heat flow analysis, indicate that the distribution of temperature throughout the depth of a superstructure is nonlinear and is a function of superstructure depth. Stresses associated with the nonlinear temperature gradients are described. These stresses can be several times those due to live load, especially in continuous systems. The stresses predicted from the idealized distributions are compared to those obtained by using the heat flow analysis. The results indicate that the idealized distributions have limited design value. Simple empirical design expressions are developed for both thermal stresses and curvature. These are based on typical climatic data for summer and winter conditions and can be applied to a variety of cross-sectional superstructure geometries. An example of the stresses induced by thermal loading on a two-span box-girder superstructure is given.

Limited data are available to assist the bridge designer concerned with the stresses induced in a concrete bridge superstructure by heating and cooling effects (1, 2, 3, 4). Current AASHTO specifications include probable temperature ranges to be used in design and generally offer guidance only with respect to expansion and contraction of straight structures. Mean temperature conditions in actual structures can differ appreciably from the ranges suggested (4, 5). No guidance is provided to designers concerned with serviceability problems in deep concrete superstructures where significant temperature differentials are possible. For example, temperature differentials approaching 22°C (40°F) (a frequently specified temperature rise) have been observed between the top and bottom of a deep (1.4-m or 4.5-ft) concrete box girder (6).

Publication of this paper sponsored by Committee on General Structures.

Some bridge design specifications or recommendations do consider differential as well as mean temperature effects (2, 3, 4). German Industrial Standard (DIN) 1072 and British Standard 153 recognize the presence of a temperature gradient through the depth of a bridge superstructure and give design values for gradients in both steel and concrete structures (3). However, little or no guidance is offered regarding the vertical distribution of the temperature differential throughout the depth of a concrete bridge superstructure. Procedures for calculating the forces and stresses induced in the superstructure by such temperature differentials are also lacking.

Why is there concern about temperature gradients in concrete bridge superstructures? Much of the design experience embodied in current specifications is based on the study of structures with both cross-sectional and plan geometries designed and constructed several years ago. The results of these studies may not be typical of superstructures currently designed and constructed. For example, concrete box girder superstructures are a recent innovation, and field observations indicate temperature differentials of more than 22°C (40°F) can exist between the upper and lower flanges of a box girder system (6). This temperature differential gives rise to local stresses that are nearly four times those attributed to full live load. Studies of a two-span prestressed concrete structure have indicated tensile stresses of more than 3450 kPa (500 lbf/in^2) directly above the intermediate support as a result of moderate temperature differentials (7). Such stress values are of importance in the design of prestressed concrete structures where cracking in the absence of live load is undesirable. Further evidence is available where damage has been attributed to thermally induced stresses (8, 9, 10, 11).

HEAT FLOW THROUGH A CONCRETE SUPERSTRUCTURE

The distribution of temperature throughout the depth of a concrete superstructure must be known if the resulting stresses, reactions, and deformations are to be calculated. It has been possible to correlate weather data with the surface temperatures of exposed pavements during heating and cooling cycles (12). However, the in-

fluence of changes in climatic conditions, with both time and location, and the factors controlling the heat gained or lost by a superstructure do not allow the direct application of the results obtained from the study of pavements to concrete superstructures.

An exposed concrete bridge deck is continually losing and gaining heat—from solar radiation, radiation to or from the sky or surrounding objects, and convection to or from the surrounding atmosphere. In the daytime, and especially during the summer, the heat gain is greater than the heat loss, resulting in a temperature increase throughout the depth. During a typical winter night, the converse is true, and the temperature in the superstructure decreases. Heat input typical of a summer day results in positive temperature gradients in the deck in which the top surface is warmer than the bottom. Negative gradients, in which the top surface is cooler than the bottom, result from a net heat loss.

The heat flow processes for typical summer and winter conditions are shown in Figure 1. Because of the poor thermal conductivity of concrete, these processes can result in temperature gradients in a concrete structure and changes in mean temperature.

Large positive temperature gradients occur during a day with high solar radiation, clear skies, a large range of ambient temperature, and a light wind. High mean temperatures, on the other hand, are associated with a high intensity of solar radiation combined with a high, almost constant, ambient air temperature. Negative temperature gradients develop during cooling periods associated with evening conditions. When the mean bridge temperature exceeds the ambient temperature at a particular time, more radiant energy is lost from the exposed top surface of a bridge superstructure than from the sheltered bottom surface.

Weather data suitable for use in a heat flow analysis considering both radiant and convective heat exchange on the upper and lower surfaces of a bridge deck vary with both time and location. Conditions at a given time and position must be considered. Observations for the months of May to August in Toronto indicate that the change in daily ambient air temperature is approximately 10°C (18°F), and the daily intensity of solar radiation on a horizontal surface has a mean value of 23 MJ/m^2 (550 langleys). Consideration of these values leads to the choice of the climatic data shown in Figure 2a as being representative of a day of high-intensity solar radiation and above-average temperature change. Similarly, data representative of a clear, still winter night in January were selected for the heat loss condition (Figure 2b).

Heat flow through a bridge superstructure varies during the diurnal cycle and is a non-steady-state process. Hence, laws governing steady-state heat flow are not applicable to exposed structures, and any analysis of the response of such structures to heat flow must consider the variation of temperature throughout the depth of the structure with time.

A one-dimensional heat flow analysis similar to that used by Emerson (5) was developed, and the resulting partial differential equation was solved by using the finite difference method. The appropriate boundary conditions considered for the heat flow analysis and the material constants assumed for the concrete are given in Table 1.

The assumption of unidirectional heat flow from the exposed surfaces of the concrete superstructure to the interior is not strictly correct. Comparisons with observed and predicted values of temperature (4, 13) indicate good correlation with unidirectional heat flow analyses, notwithstanding small transverse temperature gradients.

The application of the heat flow analysis for the representative climatic conditions (Figure 2) resulted in the temperature distributions shown in Figure 3 for solid slabs of different depths. Temperature distribution is a function of member depth for both winter and summer conditions. For the summer conditions, the surface temperatures are nearly 11°C (20°F) greater than the maximum ambient air temperature, and the temperature distribution is nonlinear for slab depths greater than approximately 30 cm (12 in). The temperature at the mid-depth of 76 and 122-cm (38 and 48-in) sections is not influenced by the exterior heat, and the change in the mean temperature of these sections is small. Winter temperature gradients do not appear to be so severe as those associated with summer conditions. Thus, a slab with a depth of more than approximately 30 cm (12 in) will, when heated or cooled as a consequence of changing radiation and temperature conditions, be subjected to nonlinear temperature distribution.

THERMAL STRESSES

A nonlinear temperature distribution and the strains associated with this gradient lead to some complexities in the computation of stresses. Structural designers do not usually consider the effect of initial strains in the analysis of sections. Figure 4 shows a typical member with an arbitrary cross section and vertical temperature distribution. The temperature varies only in the vertical direction in this analysis. Full restraint is provided to the ends of the member by the moment M and the axial force P.

A member analysis made by assuming that (a) the material is elastic and has temperature-independent properties, (b) plane sections remain plane after bending, and (c) the principle of elastic superposition is valid leads to the following equation for the longitudinal stresses $\sigma_{t,x}$ for a fully restrained member with a nonlinear temperature-induced strain

$$\sigma_{t,x} = - E\alpha\Delta T \tag{1}$$

where

$\sigma_{t,x}$ = longitudinal stress at a fiber located a distance x from the center of gravity,
α = coefficient of thermal expansion,
ΔT = change in temperature, and
E = modulus of elasticity.

The restraining end moment M can be evaluated by

$$M = - \int_{x_1}^{x_2} E\alpha\Delta T\, b_x\, x\, dx \tag{2}$$

and the longitudinal stress associated with this moment $\sigma_{m,x}$ is given by

$$\sigma_{m,x} = x\,(M/I) = -x\left(\int_{x_1}^{x_2} E\alpha\Delta T\, b_x\, x\, dx \Big/ \int_{x_1}^{x_2} b_x\, x^2\, dx\right) \tag{3}$$

where I = moment of inertia.

Similarly the restraining end force P acting on the area A and associated stress $\sigma_{p,x}$ are

$$P = - \int_{x_1}^{x_2} E\alpha\Delta T\, b_x\, dx \tag{4}$$

$$\sigma_{p,x} = P/A = -\left(\int_{x_1}^{x_2} E\alpha\Delta T\, b_x\, dx \Big/ \int_{x_1}^{x_2} b_x\, dx\right) \tag{5}$$

Figure 1. Heat gain and loss processes for (a) summer and (b) winter conditions.

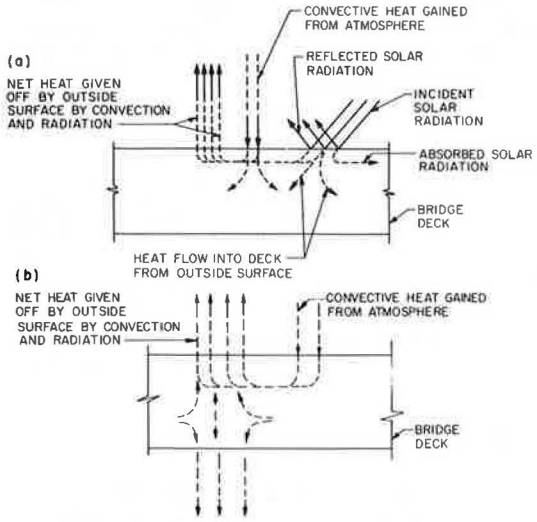

Figure 2. Typical climatic data for (a) high-intensity and (b) low-intensity radiation.

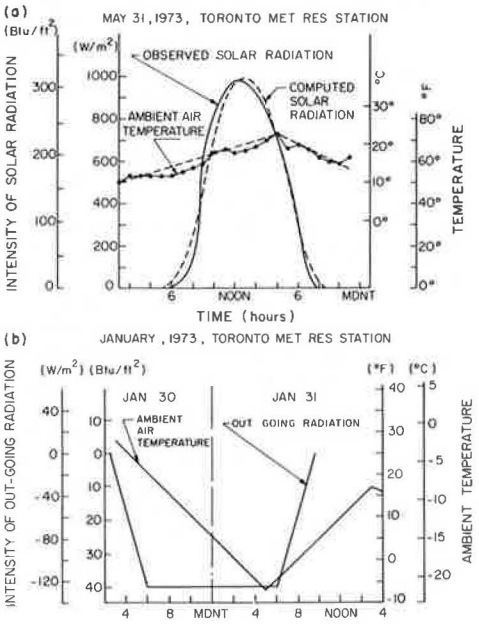

Table 1. Thermal and elastic properties used in one-dimensional heat flow analysis.

Property	Value
Diffusivity, mm^2/s	0.6
Conductivity, W/m·K	13.8
Absorptivity	
Plain concrete	0.5
Bituminous surfacing	0.9
Emissivity	0.9
Specific heat, J	242
Coefficient of expansion	0.000 010 8/°C
Top surface heat transfer coefficient, $W/m^2·K$	
Summer	23
Winter	19
Bottom surface heat transfer coefficient, $W/m^2·K$	
Summer	9
Winter	9
Elastic modulus, GPa	34.5

Note: 1 m^2/s = 10.7 ft^2/s; 1 W/m·K = 0.58 Btu·ft/h·ft^2·°F; 1 J = 0.000 95 Btu; °C = °F/1.8; 1 W/m^2·K = 0.17 Btu/h·ft^2·°F; 1 MPa = 145 lbf/in^2.

Figure 3. Typical temperature distributions during (a) summer and (b) winter.

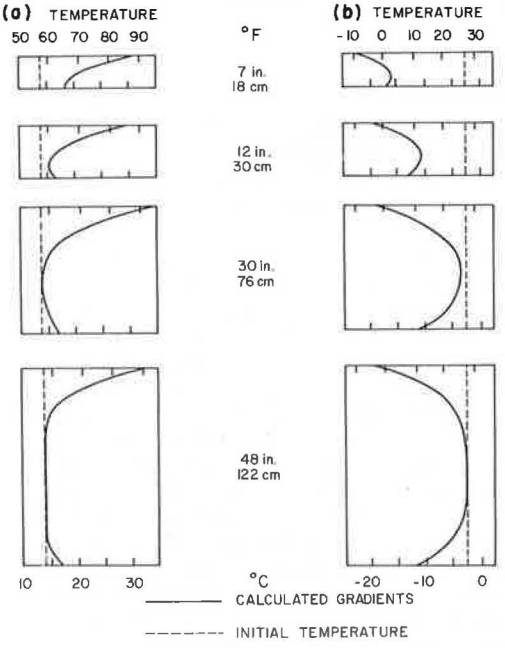

Figure 4. Restrained beam with nonlinear temperature distribution.

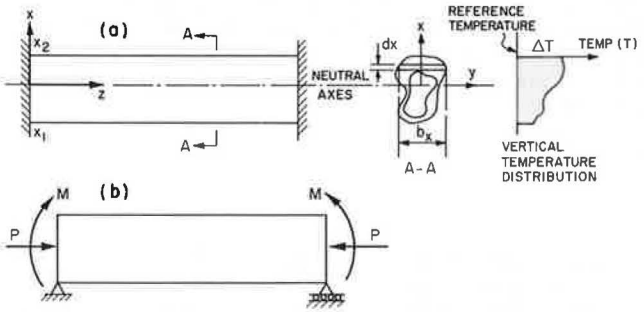

Figure 5. Sectional strains and associated stresses.

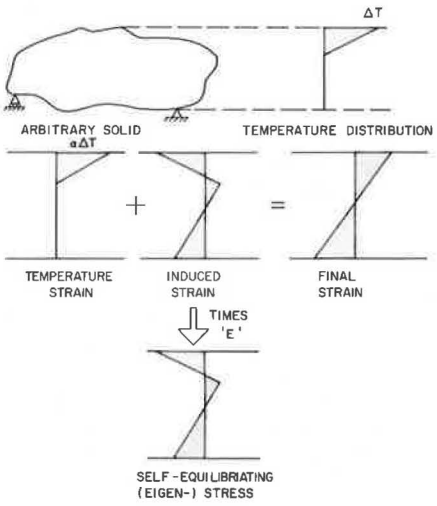

The longitudinal thermal stress σ present in a fiber located a distance x above the center of gravity of a long thin member with no end restraint (13, 14, 15) has the form

$$\sigma_{c,x} = -E\alpha\Delta T - x\,(M/I) - P/A \quad (6)$$

Subtraction of the stresses induced by the restraining forces P and M (equations 3 and 5) leads to equation 6. This latter equation describes the stress state corresponding to a nonlinear temperature gradient in an unrestrained member.

The concept of a stress state in an unrestrained member that is not subjected to external forces may be new for the bridge designer. Reference to Figure 5 may clarify this concept. The nonlinear temperature distribution attempts to induce a nonlinear strain distribution proportional in magnitude to the temperature distribution. Additional strains develop in the section as a consequence of the Euler-Bernoulli hypothesis concerning plane sections. These strains have associated self-equilibrating stresses similar in form to the residual stresses found in fabricated steel members. The self-equilibrating stresses depend directly on the daily heating and cooling cycle and material properties; they do not depend on the support conditions of a structure and, until a satisfactory English-language term is established, will be referred to as eigen stresses.

If the curvature of a member induced by a temperature gradient is restrained by the interior supports of a continuous beam, additional stresses develop. These additional stresses will be referred to as continuity stresses, and the form of the moments and reactions associated with these stresses is shown in Figure 6. The value of maximum thermal continuity stress for the two-span beam is

$$\sigma_{c,z} = {}^3/_2\phi Ec \quad (7)$$

where

$\sigma_{c,z}$ = continuity stress at the support,
ϕ = thermal curvature, and
c = distance to the extreme fiber from the centroidal axis,

and, in general,

$$\sigma_{c,z} = C_1C_2\phi dE \quad (8)$$

where

C_1 = constant developed from the span geometries (1.5 for a two-span system, 1.0 for the interior span of a multispan system),
C_2 = constant developed from the sectional geometry (0.5 for a rectangular section), and
d = member depth.

The total stresses developed in a two-span member for typical summer and winter conditions (Figure 7) consist of both eigen stresses and continuity stresses. As mentioned previously, the eigen stresses are self-equilibrating stresses formed as a consequence of the nonlinear temperature distribution throughout the section depth, and continuity stresses develop because the deflection at point B (Figure 7) is zero. Inspection of the total stress patterns (Figure 7a) indicates that large tensile stresses develop in the web of the member as a consequence of the summer conditions.

Thus, a prestressed concrete member designed for zero tension at support B under dead load plus prestress should be provided with reinforcing steel in the web to cater for these thermally induced tensile stresses. Leonhardt has also noted this requirement based on a simpler analysis (7). Well-distributed steel is required in the flange to cater for the tensile stresses due to the winter condition (Figure 7b).

It is apparent from Figure 6 that summer heating effects change the values of reaction. Some experimental data are available describing reaction change for a three-span bridge, but regrettably values of the intensity of incoming solar radiation were not available (16). Typical values were assumed, and the reaction changes calculated from derived curvature values appear to predict the observed values closely for a day with high solar radiation (18). The observed reaction change results in a moment change of nearly 60 percent of the dead load moment for the double girder three-span structure with spans of 13, 17, and 13 m (44, 55, and 44 ft).

DESIGN CONSIDERATIONS

In the literature, several temperature distributions have been suggested for design (7, 14, 17). The adequacy of these distributions with respect to the prediction of eigen stress and continuity stress values in concrete superstructures does not seem to have been examined previously. Figure 8 shows several suggested temperature distributions. The eigen stresses and curvature values induced by these distributions were computed for summer conditions. It is apparent that the form and magnitude of both the eigen stresses and curvatures are strongly dependent on both assumed temperature difference and temperature gradient. Linear gradients do not induce eigen stresses. Temperature measurements obtained from prototype structures with depths of approximately 1 m (3 ft) correspond most closely to those predicted by a sixth-degree parabola (5). The stresses corresponding to this distribution are very similar in magnitude and distribution to those recommended by Maher, who considers a linear gradient throughout the depth of the top slab of a box girder superstructure (17). The temperature difference (23°C or 40°F) used in the example should be considered as an upper limit (6).

Three representative temperature distributions and the one-dimensional heat flow analysis were used to compute eigen stresses and nondimensional curvatures (ϕd) for various depths of a solid slab. The distributions used and the results obtained are given in Figures 9 and 10. Not all concrete superstructures are solid, and corrections to the analysis for cellular structures are available (18).

Two values of temperature differential (10 and 20°C or 18 and 36°F) were considered for the linear gradient (the Leonhardt gradient). For the Priestley and Maher gradients, a temperature differential of 19°C (35°F) was used. The linear Maher gradient was assumed to extend to 20 cm (8 in) below the surface of the solid superstructure. The sixth-order parabolic distribution suggested by Priestley (14) was used.

Figure 9 shows that the Maher distribution and one-dimensional analysis compare favorably for the prediction of eigen stress values for a wide range of depths. The Priestley distribution appears to have a limited range of applicability, and eigen stresses cannot be predicted by using a linear temperature distribution. The nondimensional curvature versus depth predictions (Figure 10) show that the Maher distribution will overestimate curvature compared to the one-dimensional analysis for shallow members; the Priestley distribution applies only to member depths of between 0.75 and 1.0 m (30 to 40 in), and the Leonhardt distribution is indepen-

Figure 6. Restrained curvature of a member with (a) no temperature gradient, (b) induced curvature, (c) applied loading, and (d) final moments and reactions.

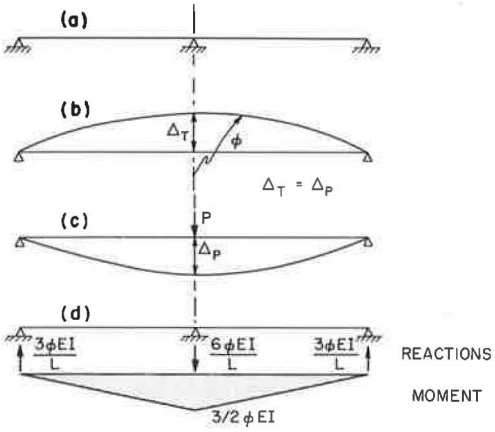

Figure 7. Two-span beam under (a) summer and (b) winter conditions.

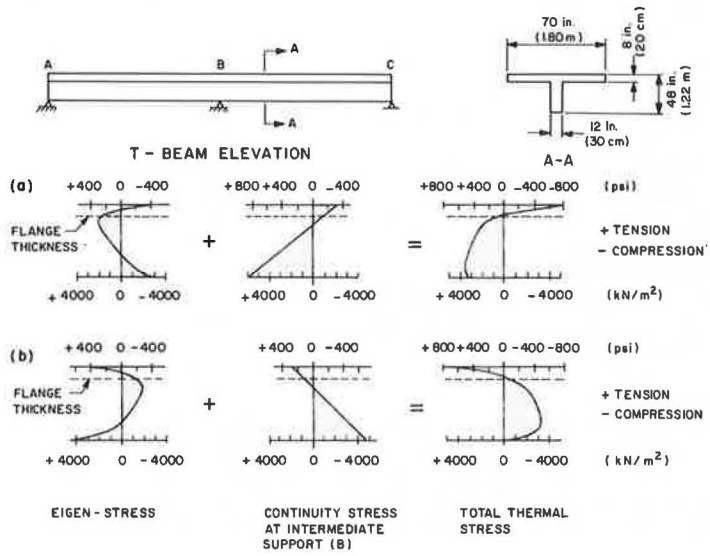

Figure 8. (a) Temperature distributions and resulting (b) eigen stresses and (c) curvature values.

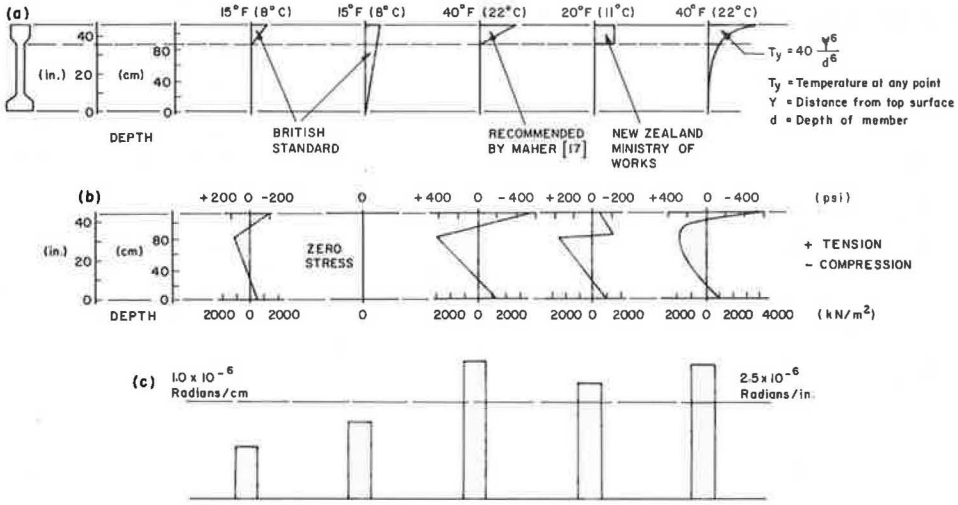

Figure 9. Eigen stress comparisons for various distributions and depths.

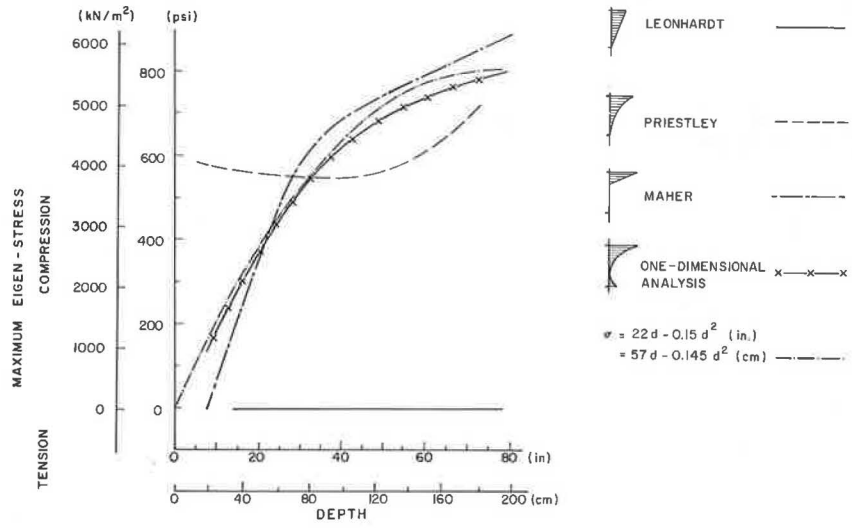

dent of member depth, contrary to the Maher and one-dimensional analysis predictions.

For design purposes, the calculation of the eigen and continuity stresses associated with a given temperature distribution would be tedious. Simple empirical design expressions were developed from Radolli's analyses (18) for use as first approximations in design. The results for summer heating conditions are given in Figures 9 and 10 and allow calculation of both eigen stresses and nondimensional curvature for various depths of slab with relative ease. For depths less than 50 cm (20 in), the nondimensional curvature is assumed to be constant. These expressions are based on climatic conditions for Toronto and are therefore valid for locations of similar climate.

Figures 9 and 10 can be used to predict values associated with winter conditions. It was found that eigen stress values for winter heat flow conditions are nearly identical to the values for summer conditions but of opposite sign; also curvature values are of the opposite sign and are only 60 percent of the summer values. Thus, one set of simple calculations can be used to obtain the stress values associated with thermal loading for both summer and winter conditions.

The results presented apply to a variety of cross-sectional geometries including cellular and T-beam sections (18, 19). Variations in material properties and heat transfer coefficients will influence stress values. However, the changes in the stress values for a wide range of properties and coefficients were found to be within 25 percent of the values presented here (18).

Figure 10. ϕd for various distributions and depths.

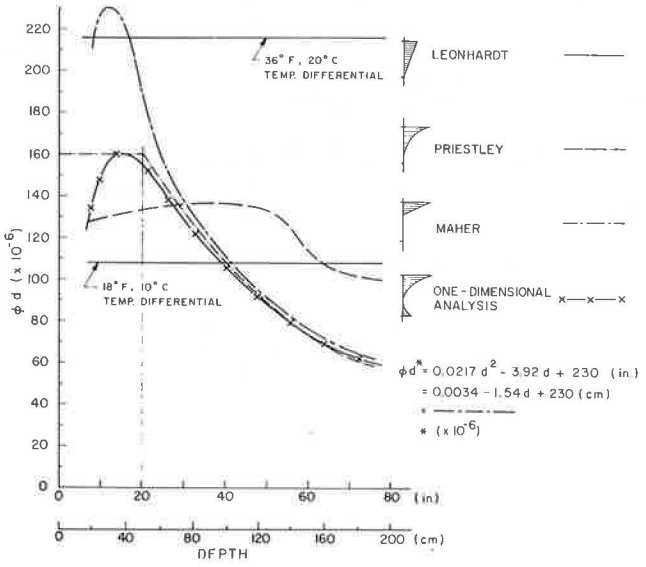

Figure 11. Observed and computed temperature gradients during (a) summer and (b) winter.

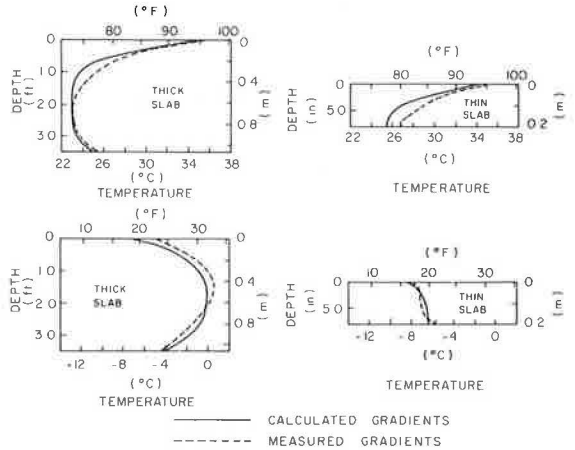

DISCUSSION OF RESULTS

The analyses and results presented for stress are based in part on a one-dimensional heat transfer analysis for a solid slab. A comparison of measured and computed temperature values (Figure 11) confirms the general validity of the analysis.

The effect of thermal loadings associated with summer conditions on the design stress envelopes for typical concrete bridge superstructures has been discussed (19). Figure 12 provides an example of the stresses developed in a two-span posttensioned box girder as a consequence of winter cooling conditions. Surface tensile stresses develop throughout the length of the structure as a consequence of the nonlinear temperature distribution. These tensile stresses influence both the span and support regions of the structure. The serviceability of such a box girder structure could well be affected if additional bonded reinforcing steel is not added for crack control in zones of high tensile stress.

Thermal loadings will not affect the overall strength

Figure 12. Stresses in a box girder bridge: (a) bending moment due to thermal load, (b) total thermal stress, (c) live load and impact stress, and (d) total working stress.

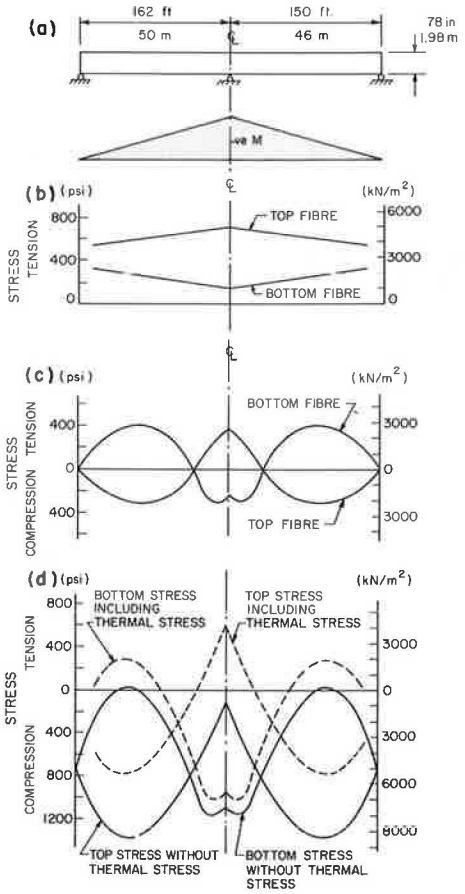

of a continuous superstructure inasmuch as failure of the superstructure will result in a release of the restraints causing thermal stresses. However, heating and cooling of the structure during a normal diurnal cycle combined with lifetime creep and shrinkage must be considered in the serviceability analysis of concrete superstructures.

CONCLUSIONS

Significant flexural stresses are developed in concrete bridge superstructures as a consequence of the heating or cooling of concrete—a material of relatively poor thermal conductivity. Nonlinear temperature gradients develop during a daily heating or cooling cycle. These gradients lead to both eigen and continuity stresses. Simple design formulas are developed that allow the prediction of these stresses and do not require a knowledge of the temperature gradient.

Thermal loading of a superstructure is a serviceability problem and should be so considered. Proportioning of reinforcement in a concrete bridge superstructure should reflect the stress-inducing thermal effects.

ACKNOWLEDGMENTS

The work was carried out with the support of the Transportation Development Agency of Canada, the National Research Council of Canada, and the Department of Civil Engineering, University of Waterloo. This support is gratefully acknowledged.

REFERENCES

1. Standard Specifications for Highway Bridges, Eleventh Ed. AASHO, Washington, D.C., 1973.
2. Design of Highway Bridges. Canadian Standards Association, Rexdale, Ontario, CSA Standard S6-1974, 1974.
3. D. J. Lee. The Theory and Practice of Bearings and Expansion Joints for Bridges. Cement and Concrete Association, London, 1971.
4. M. Emerson. Bridge Temperation and Movements in the British Isles. U.K. Road Research Laboratory, Crowthorne, Berkshire, England, RRL Rept. LR228, 1968.
5. M. Emerson. The Calculation of the Distribution of Temperature in Bridges. U.K. Transport and Road Research Laboratory, Crowthorne, Berkshire, England, TRRL Rept. LR561, 1973.
6. H. Bosshart. Thermal Stress in Prestressed Concrete Bridges. Symposium on Design of Concrete Structures for Creep, Shrinkage and Temperature Changes, Madrid, Final Rept., Vol. 6, 1970, pp. 73-80.
7. F. Leonhardt and W. Lippoth. Folgerungen aus Schäden an Spannbetonbrücken. Beton-und Stahlbetonbau, Vol. 65, No. 10, Oct. 1970, pp. 231-244.
8. J. N. Deserio. Thermal and Shrinkage Stresses—They Damage Structures! ACI, Detroit, Publ. SP27, 1971, pp. 43-49.
9. T. Monier. Cases of Damage to Prestressed Concrete. Heron, Vol. 18, No. 2, 1972.
10. K. H. Weber. Causes of Crack Formation Near Intermediate Supports of Continuous Prestressed Concrete Beams and Their Limitations to Allowable Crack Width. Univ. of Stuttgart, dissertation, 1967.
11. R. D. Larrabee, D. P. Billington, and J. F. Abel. Thermal Loading of Thin-Shell Concrete Cooling Towers. Journal of Structural Division, Proc., ASCE, Vol. 100, No. ST12, Dec. 1974, pp. 2367-2382.
12. E. S. Barber. Calculation of Maximum Pavement Temperature From Weather Reports. HRB, Bulletin 168, 1957, pp. 1-8.
13. W. I. J. Price and R. G. Tyler. Effects of Creep, Shrinkage and Temperature on Highway Bridges in the United Kingdom. Symposium on Design of Concrete Structures for Creep, Shrinkage and Temperature Changes, Madrid, Final Rept., Vol. 6, 1970, pp. 81-93.
14. M. J. N. Priestley. Effects of Transverse Temperature Gradients on Bridges. New Zealand Ministry of Works, Central Laboratories, Rept. 394, Oct. 1971.
15. R. Hoyle. Plane Strain and Plane Stress. In Thermal Stress, Pitman and Sons, London, 1964, pp. 43-51.
16. N. Krishnamurthy. Temperature Effects on Continuous Reinforced Concrete Bridges. Alabama Highway Research, HPR Rept. 58, July 1971.
17. D. R. H. Maher. The Effects of Differential Temperature on Continuous Prestressed Concrete Bridges. Institution of Engineers, Australia, Civil Engineering Trans., Vol. CE12, No. 1, Paper 273, April 1970, pp. 29-32.
18. M. Radolli. Thermal Stresses in Concrete Bridge Superstructures. Univ. of Waterloo, Ontario, MASc thesis, March 1975.
19. M. Radolli and R. Green. Thermal Stress in Concrete Bridge Superstructures Under Summer Conditions. TRB, Transportation Research Record 547, 1975, pp. 23-36.